

INTERPOLATION AND 3D VISUALIZATION OF SOIL MOISTURE

ANDRÁS HERVAI^{1*} – ERVIN PIRKHOFFER² – SZABOLCS ÁKOS FÁBIÁN²
– ÁKOS HALMAI³ – GÁBOR NAGY¹ – DÉNES LÓCZY² –
SZABOLCS CZIGÁNY²

¹Doctoral School of Earth Sciences, Faculty of Sciences, University of Pécs, Ifjúság u. 6. Pécs, 7624, Hungary;

²Department of Physical- and Environmental Geography, Institute of Geography, Faculty of Sciences, University of Pécs, Ifjúság u. 6. Pécs, Hungary;

³Department of Cartography and GIS, Institute of Geography, Faculty of Sciences, University of Pécs, Ifjúság u. 6. Pécs, 7624, Hungary

*corresponding author, email: ahervai@gamma.ttk.pte.hu

Abstract

Adaptation to climate change demands the optimal and sustainable water management in agriculture, with an inevitable focus on soil moisture conditions. In the current study we developed an ArcGIS 10.4. platform-based application (software) to model spatial and temporal changes in soil moisture in a soy field. Six SENTEK Drill & Drop soil moisture sensors were deployed in an experimental field of 4.3 hectares by the contribution of Elcom Ltd. Soil moisture measurement at each location were taken at six depths (5, 15, 25, 35, 45 and 55 cm) in 60-minute intervals.

The model is capable to spatially interpolate monitored soil moisture using the technique. The time sequence change of soil moistures can be tracked by a Time Slider for both the 2D and 3D visualization. Soil moisture temporal changes can be visualized in either daily or hourly time intervals, and can be shown as a motion figure.

Horizon average, maximum and minimum values of soil moisture data can be identified with the built-in tool of ArcGIS. Soil moisture spatial distribution can be obtained and plotted at any cross sections, whereas an alarm function has also been developed for tension values of 250, 1,000 and 1,500 kPa.

Keywords: 3D numeric modelling, soil moisture, water management, liquid limit according to Arany

1. Introduction

Preparation for climate change demands optimal and sustainable water supplies for cost-efficient and sustainable agricultural productivity (Makó et al. 2010), which requires the thorough understanding and sound knowledge on vadose zone soil moisture conditions. Soil moisture is a highly variable environmental parameter, both spatially and temporally (Loew – Schlenz 2011), and knowledge on its spatial heterogeneity may provide useful

information for precision farming and cost-efficient crop production (Paul – Speckmann 2004).

Soil moisture spatial distribution varies both vertically and horizontally in a small scale largely due to topography (Anderson – Kneale 1980; Zhu – Lin 2011), soil texture, soil organic matter content and vegetation (Novák 2005; Novák et al. 2013). Principal options to obtain sufficient knowledge on spatial distribution of soil moisture include high resolution ground monitoring (Zhu – Lin 2011; Bárdossy – Lehmann 1998) or satellite

remote sensing applications (Jia et al. 2013; Penna et al. 2009; Mohanty – Skaggs 2001). A relatively few papers are available on in situ measurement with sensors, whereas a large number of studies tested remote sensing data on large-scale soil moisture products. One drawback of the remote technique is that it only obtains data from the very shallow subsurface in limited depth (max.: 15-20 cm) (Brocca et al. 2009; Heathman et al. 2012) and is more applicable for larger area than on plot-scale or small watersheds (Hegedüs et al. 2015). Other factors that limit radar technology measurement comprise bulk density, surface roughness and high vegetation density. Radar soil moisture measurements may also be biased due to frequency shifts and loss in power of a radar signal (Paul – Speckmann 2004). Precision can be further reduced by background signal disturbances (spreading, attenuation, reflection and scattering) and flight density (Zhou et al. 2016).

Nevertheless, the use of ground soil moisture measurements, at least in high spatial density, is costly and labor-intensive. If the correlation is sufficiently robust, a single soil moisture sensor could provide the necessary input to predict soil moisture across the watershed (Wang – Qu 2009; Venkatesh et al. 2011; Cosh et al. 2004), assuming that the environmental variables (i.e. land use and soil characteristics) remain unchanged (Lacava et al. 2010). Such predicted datasets within the watershed may provide sufficiently accurate soil moisture (Fu et al. 2003; Loew – Schlenz 2011; Bárdossy – Lehmann 1998). When multiple sensors are needed for the studied area, to overcome the challenge of cost-efficiency, measured data should be interpolated among the measurement points through correlation functions with various GIS applications (Gravalos et al. 2013). A large number of interpolations techniques, methods and functions have been used to estimate soil moisture among the measurement points (e.g.: Yao et al. 2013). Yao et al. (2013) tested four different interpolation methods,

namely the ordinary kriging, inverse distance weighting, linear regression and regression kriging. According to their results the latter performed the best. Perry and Niemann (2008) used empirical orthogonal functions to estimate soil moisture among measurement points.

Nonetheless, most interpolation models focused on 2-dimensional distribution of soil moisture, and only a limited number of publications are available on 3D-modelling, most commonly using Hydrus-3D, which, in most cases performed well (Honar et al. 2011). Gravalos et al. (2013) developed a soil moisture interpolation model under laboratory circumstances. In their soil tank they measured soil moisture in a depth of 15 cm. Although their model performed well at laboratory-scale, data interpretation at field scale is challenging.

Our objective was to develop a relatively simple and cost-efficient 3-dimensional soil moisture visualization software which is suitable to present the moisture dynamics of multiple soil layers and horizons in real time. We aimed to indicate the temporal changes of soil moisture in each soil master horizons and project and interpolate data at plot scale (few hectares). We also planned to create a plotting function that is capable to show and visualize temporal changes of soil moisture in any arbitrarily selected point in space (including interpolated points). The result of the research is the property of Elcom Ltd.

2. Materials and methods

Site description

The study area (Koppló Plot) is located on the southern foothills of the SW part of the Mecsek Hills (Jakab-hegy) in SW Hungary (Fig. 1.). The plot is owned by B-Aranykorona Ltd., and was followed from mid-July to mid-September, when rape was planted in the plot. The study site covers a land area of 4.3 hectares and is characterized by Ramann-type brown forest soils (WRB: Stagnic Cambisol).

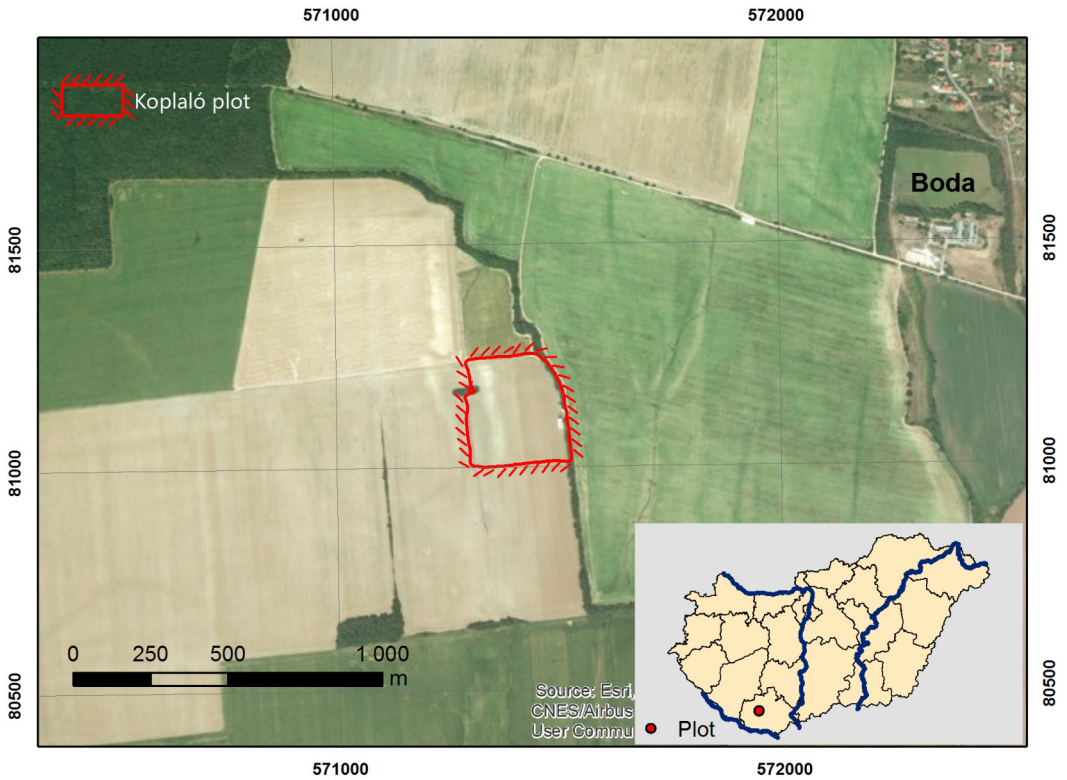


Fig. 1. Location of the study site

The elevation ranges between 171.85 and 182.76 meters a.s.l. with a maximum slope of 5.41% on the southern, south-western steep, a former foothill colluvial deposits (Fig. 2.). The long-term (1971–2000) average annual

precipitation total is 700 mm with most rainfall measured between May to mid-July (295 mm), when the precipitation regime is characterized by high-intensity convective rainfall events.

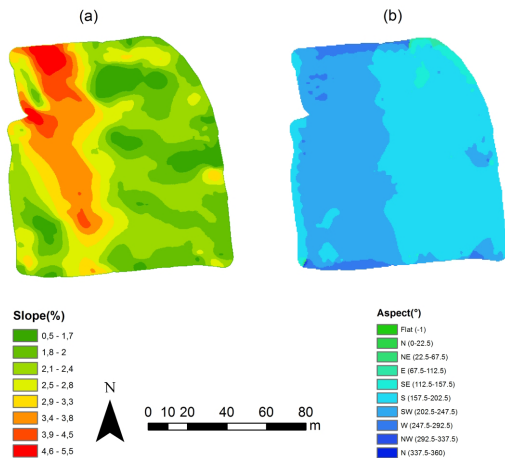


Fig. 2. (a) Slope and (b) aspect map of the study area (Koplaló Plot)

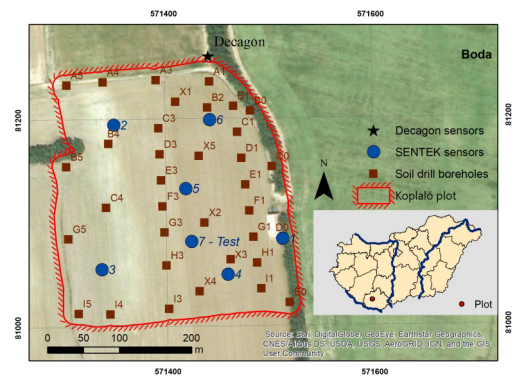


Fig. 3. Location of the soil moisture sensors (SENTEK and DECAGON) and the borehole sampling sites

Based on our field measurements, using a TOPCON HiPer Pro (Topcon Positioning Systems, Inc., Tokyo, Japan) RTK GPS device, a digital elevation model (DEM) of a meter horizontal resolution was developed in ArcGIS 10.4. software environment.

Soil moisture monitoring and soil sampling

In July, 2016 a soil profile of 150 cm depth was excavated to identify master horizons and for soil sampling purposes about 30 meters north of the northern borderline of the studied plot. Soil samples were taken in three repetitions from each master horizon (Ap, A, B, BC and C) with Veér-type brass rings with a volume of 100 cm³ and a diameter of 48 mm at depths of 15, 25, 50 and 115 cm to determine bulk densities and soil moisture with the gravimetric method according to Flint – Flint (2002). Four Decagon 10HS sensors (Decagon Devices Inc., Pullman, WA, United States) and four MPS-2 in one profile at the norther edge of the experimental plot (Fig. 3.) were inserted into depths of 15, 25, 50 and 115 cm. Sensors were deployed on July 18, 2017 and data have been collected since then continuously in 30-minute intervals with a Decagon EM50 datalogger to obtain the water retention curves for the aforementioned soil depths

Soils of the studied plot were sampled with an AMS hand sampling tool at 35 locations to a depth of maximum 290 cm and at one point, at the northern border of the plot a soil profile was excavated to a depth of 120 cm to identify the major soil horizon and to insert the Decagon 5TM and MPS-2 sensors. The soil sampling size were first positioned according to a standardized grid method with equal distances (2×8 drilling holes in North-South direction), second, at the margins (2×4 holes) in order to get an interpolation surface and then 11 randomly located intermediate points were sampled. The depth and thickness of each master soil horizons (Ap, A, B, BC and C) were determined at all sampling sites. Soil samples were taken at each sampling site from all master horizons,

therefore altogether 175 soil samples were collected.

Six SENTEK Drill & Drop (Campbell scientific, Edmonton, Alberta, Canada) soil moisture sensors were deployed in an experimental field of 4.3 hectares. Soil moisture measurement at each location were taken at six depths (5, 15, 25, 35, 45 and 55 cm) in 60-minute intervals.

A seventh SENTEK sensor was deployed for data validation purposes on March 18, 2017, positioned at E571509.615 m, N81110.308 m (Unified National Projection System, EPSG: 23700).

Laboratory analyses

To determine soil textural classes, the liquid limit according to Arany were determined according to Buzás (1993). Soil texture was also determined with a dynamic light scattering method using a Malvern MasterSizer 3000 (Malvern Inc. Malvern, England, UK) particle size analyzer. Samples were pretreated with 10% HCl for CaCO₃ and with 10% H₂O₂ for organic matter removal.

Walkley-Black titration for organic carbon with 0.1n K₂Cr₂O₇ as an oxidizing agent was used, while 96% H₂SO₄ was used to extract organic matter (quantification). Color intensity was determined with a Biochrom Libra Spectrophotometer (Biochrom Ltd. Cambridge, England) at the wavelength of 585 nm.

Development of the DEM for each master horizon

After generating the surface DEM, we delineated the surfaces of each soil horizons (Ap, A, B, BC, C). Master horizon depths were imported line-by-line into an ArcGIS geodatabase table. Then string-like stitches were strung on soil drilling point feature classes (by the Make Route Event Layer geoprocess function) from the different depth data of the table. From the Z values of the points, raster surfaces were made with the Spline geoprocess function. Since the raster surfaces cannot be extruded into

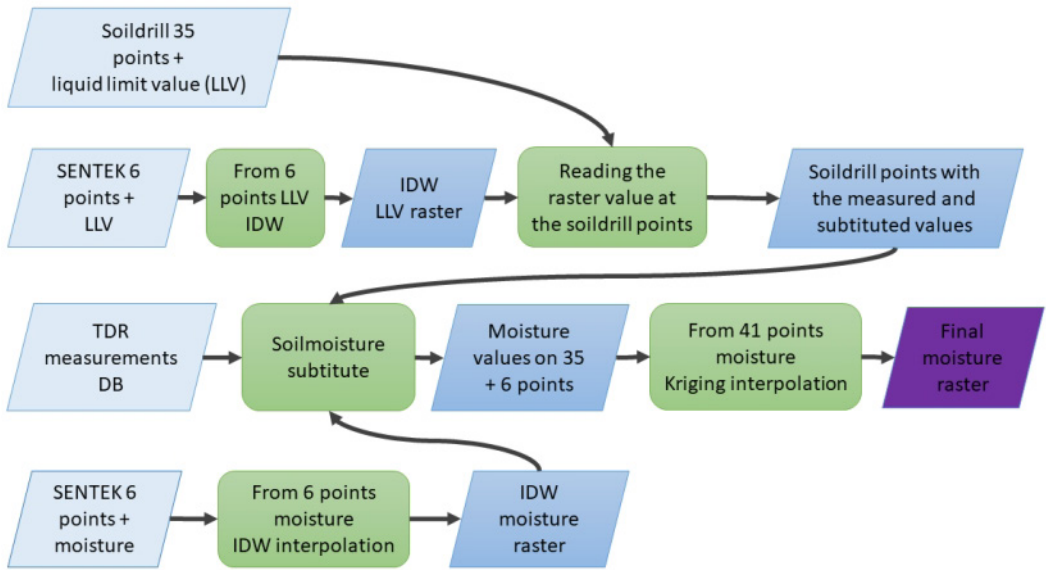


Fig. 4. Soil moisture interpolation process

three-dimensional layers (multipatch), TIN surfaces were generated with the Raster To Tin geoprocess function from the raster maps generated by Spline.

Between the adjacent TIN layers, each soil horizons were generated with the ArcGIS Extrude Between geoprocess function. The extruded three-dimensional layers (multipatch) from the TIN generated irregularities (iridescence) at their edge. This phenomenon occurs when the edges of the soil layers are not perfectly smooth. To resolve this error, we used the Buffer geoprocess function to make the TIN layers 5 percent wider. Using the functionality of Extrude Between geoprocess function, we gave the original basemap (Area of Interest - AOI) as boundary. Thus, each soil layer extent from top view deepens according to the base map beneath the different surfaces (Fig. 7.). For the three-dimensional display, however, we had to vertically exaggerate each layer downward to make the layers visually interpretable.

Interpolation of soil moisture values

Based on its suitability on soil moisture interpolation the ordinary kriging technique

for interpolation was used. As long as deterministic functions interpolate with one exact value of the measured point, the geostatistical functions utilize the statistical properties of the measured point. Deterministic interpolation techniques create surface from the measured points, based on either the extent of the similarity (inverse distance weighted) or the degree of the smoothing (spline).

As a first step soil moisture can be interpolated with IDW technology at each time step (hour and day) in each depth (5, 15, 25, 35, 45, 55 cm) based on soil moisture values measured by six SENTEK Drill&Drop sensors (Fig. 4.).

The result raster map has a quite bad resolution. However, we know the liquid limit value according to Arany of the given 6 different depths of the 6 sensor (Fig. 5.). From these values a raster map can also be created still with IDW type interpolation.

Soil samples were taken at 35 locations in the field and the liquid limit value according to Arany at each genetic soil horizon of the 35 points were determined under laboratory conditions (Fig. 6.). Samples were collected at the measurement depths of the SENTEK

sensors (5, 15, 25, 35, 45, 55 cm). We also read the liquid limit IDW raster value at each soil drilling point and added it to their feature class as an attribute.

Soil moisture data were collected with a manual soil moisture meter (Spectrum TDR-300) in the sample plot from the soil horizons with different liquid limit values seven times between the summers of 2016 and 2017. The data were inserted into a table (Fig. 4.). In each depth of soil drillings, the soil moisture IDW interpolated values were also saved. Based on our table we changed the soil moisture values.

For the development of the interpolated raster, as an example, if the IDW calculated liquid limit value of the H3 borehole at a depth of 5 cm (Fig. 6.) was 46 and the moisture value was 21.4% then we looked at the percentage of moisture at liquid limit value 43 in our table based on the predefined functions. This new moisture value (23.9%) was also saved as an attribute for each depth of the given drilling. We measured moisture values for 41 points (at six different depths). These 41 points were interpolated again by ordinary kriging technique, which requires a minimum number of 30 data points (Or-Wraith 2000).

An alarm function has also been developed for the model, with four categories, with threshold values at tension values of 1,500

(permanent wilting point), 1,000 and 250 kPa. The moisture content – water potential relations were generated with water retention curves based on measured data and fitted with RETC 6.02 using the van Genuchten-Mualem relationship (van Genuchten 1980; Maulem 1976).

Transformation of raster maps into vector maps

Raster maps are easily used for visualization, whereas date attribute cannot be as easily assigned as to vector files. Since we aimed to visualize temporal changes of soil moisture, small vector files were needed (80-90 kB). Firstly, we created the contour lines of the time interval raster maps with the help of Contour geoprocess function then we bounded around polygons from contour lines with the Feature To Polygon geoprocess function. We projected the center of polygons onto the original raster and read out the corresponding soil moisture value. In other words, we generalized soil moisture spatial data by converting raster-based maps to vector maps that are 20 times smaller in size than the corresponding raster files. The completed polygon map allows the real-time motion of time sequence of long-term soil moisture. The soil moisture polygons of different depth were then merged for the entire measurement period to obtain real-

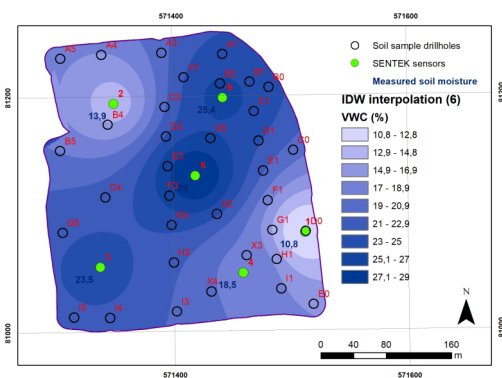


Fig. 5. Volumetric Water Content IDW interpolation in 5 cm depth based on value measured by SENTEK sondes

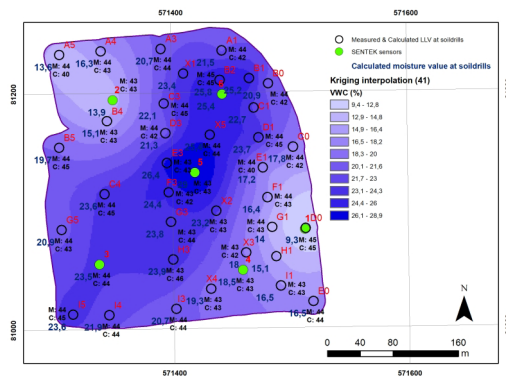


Fig. 6. Volumetric Water Content Kriging interpolation in 5 cm depth based on value measured by SENTEK sondes and calculated for soil drill points

Table 1. Characteristics of soil layers

Horizon name	Average extent (cm)	Characteristics
Ap	0-10	Deep plow is not typical
A	10-35	More clay content than Ap layer, contains a lot of humus
B	35-60	Clay accumulation based on observed field surveys
BC	60-100	Gradually passes through the top and bottom levels
C	100-200	Soil-forming rock is pale yellow loess

Table 2. Mean, maximum and minimum soil moisture values (%) measured over the monitored period

Depth (cm)	Min	Max	Avg	Std
5	6.07	29.90	16.05	5.53
15	19.03	37.94	29.22	4.97
25	26.95	41.527	36.38	4.13
35	33.35	43.72	40.21	2.50
45	35.64	42.10	39.35	1.50
55	36.58	41.49	39.21	1.16

Table 3. Threshold volumetric water contents for the alarm function at 250, 1,000 and 1,500 kPa tension values

Horizon name	Threshold volumetric water contents for alarm ($\text{m}^3 \text{m}^{-3}$)		
	250 kPa	1,000 kPa	1,500 kPa
Ap	0.176	0.152	0.146
A	0.174	0.150	0.123
B	0.174	0.151	0.146
BC	0.138	0.124	0.121

time vector files that are movable both in time and space.

2D view of soil moisture values in ArcMap

We also created the top view time sequence for any single master horizons in ArcMap in order to be able to follow each point of each depth of soil moisture values. Soil moisture vector maps calculated for different depths were placed spatially shifted by 300 meters in to the east (EOV Easting 300) while 600 and 1200 meters to the south (EOV Northing -600, -1200). This way moisture pattern of each master horizons was visualized at the same time, however only the map in the upper left corner kept its actual position (Fig. 10.).

3. Results

Soil data

According to our field soil survey and the subsequent laboratory analyses silt

fraction dominated the soils of the studied plot. Genetic soil type was classified as Ramann-type brown forest soils (WRB: Stagnic Cambisol), with clay illuviation in the B-horizon and with occasional stagic properties. Ap horizon typically ranged between 7 to 12 cm indicating only shallow tillage operations. Depth of the parent material (Pleistocene loess) from the ground surface varied between 50 and 290 cm, depending on hill position, identified as Colluvic Regosol (Table 1). The measured Arany values well correspond with the former measurements (KA = 34–47) carried out by the MINERAG Ltd. and prepared for landowner B-Aranykorona Ltd. For the 35 soil samples taken with borehole drillings, the liquid limits according to Arany ranged between 37.65 and 50.9, with a mean value of 43.8, indicating loamy and clay loam texture for most of the soil samples.

This west margin of the pediment is clearly an accumulation ground where soil sediment is continuously deposited from the uphill part

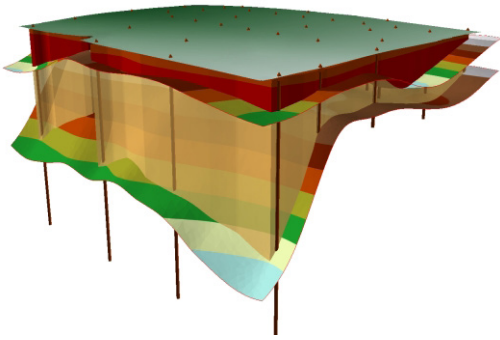


Fig. 7. Depth of the master horizons (50× vertical exaggeration) and the location of the soil sampling boreholes

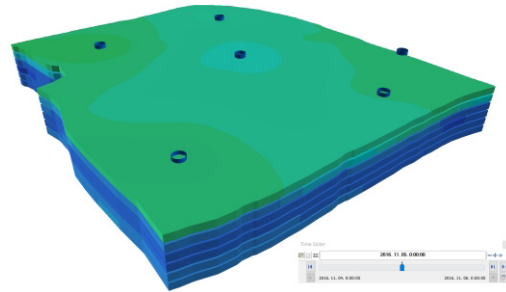


Fig. 8. The interpolated soil moisture layers with the Time Slider application in ArcGIS ArcScene (50×vertical distortion)

of the plot, which is typically characterized by shallow topsoils with a depth less than 60 cm to the top of the C-horizon. Intense rainfall events, due to gully erosional processes, has carved 50-100 cm deep erosion gully into the valley-bottom. Variations in topsoil depths were identified by drilling data. Horizon depth are shown and visualized in the interpolated 3D model (Fig. 4.).

Soil moisture values over the monitoring period ranged between 6.07 and 43.72% whereas water potential reached its lowest value (-2163 kPa) on October, 3, 2016. The field and laboratory measured soil physical properties formed an integral part of the

soil moisture interpolation model, and all measured data have been inserted and employed in the model.

Main characteristics of the obtained software

The current version of the software has a 2D and 3D visualization module, that can be viewed in ArcGIS ArcMap (v. 10.4) and ArcScene (v. 10.4), respectively. Mandatory input data include name and depths of master soil horizons, number, location (in X, Y Hungarian Unified National Projection System) and depth of soil moisture sensors, liquid limits according to Arany, water

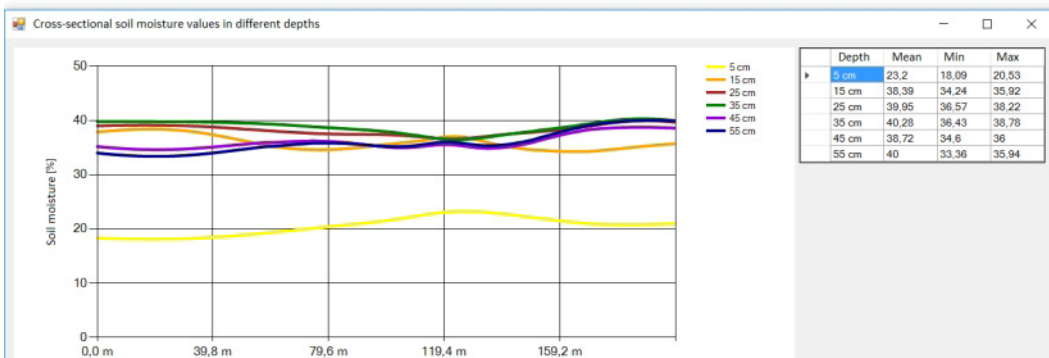
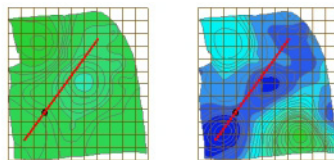


Fig. 9. Spatial distribution of soil moisture at the six measurement depths (shifted horizontally for complete and simultaneous display). Soil moisture values (θ_v) are indicated in % ($=m^3 m^{-3} \cdot 100$)

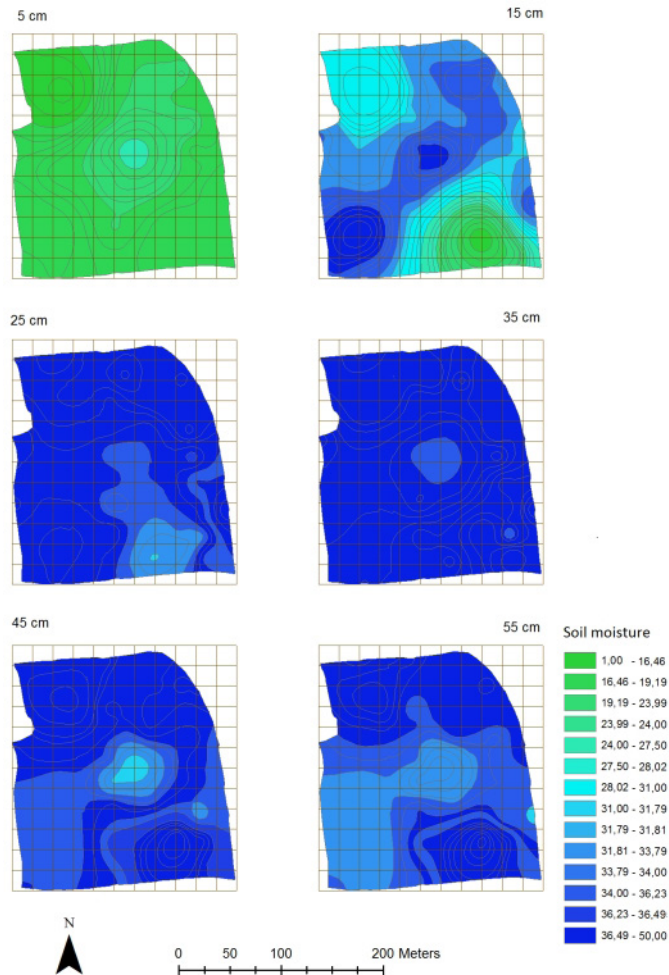


Fig. 10. A cross-sectional view of soil moisture at a selected time

retention curves and organic matter content for each master horizon (%). Data can be either typed or imported from Excel. Entered topography and soil horizon elevation and depth data can then be directly visualized in the program (Fig. 7.).

In the current version only ordinary kriging is available as interpolation technique. Soil moisture can be shown for any master horizon of the given soil. The time sequence change of soil moistures can be tracked and visualized by a Time Slider for both the 2D and 3D visualization (Fig. 8. and 9.). Soil moisture temporal changes can be visualized in either daily or hourly time intervals for

any selected point in space within the area of interest, and can be shown as a motion figure. With the ArcScene on-the-fly function, soil moisture pattern in soils of complex structure and layering can be analyzed and explored. Horizon average, maximum and minimum values of soil moisture data can be identified with the built-in tool of ArcGIS. Cross-sectional data in any directions can be obtained and plotted on a graph (Fig. 10.).

The alarm function has four categories in the model denoted with red, yellow, orange and green colors. Threshold volumetric water contents are shown in Table 3.

4. Discussion

In the current study we have developed a measurement-based simple numeric soil moisture calculation and 2D and 3D visualization model. The model is applicable for many nature conservation and crop yield optimization projects, without complex calculations (e.g.: Richards equation). The software interpolates soil moisture data based on clay content of the soils and is capable to visualize data in two- and three-dimensional GIS software environment. We are aware that applicability of described method is limited as it requires spatially detailed measurement of soil texture and soil type. Soil moisture interpolation models may also serve as a substitute for spaceborne radar analyses or rather as a verification tool to validate remotely sensed data. Although a large number of uncertainties are related to soil moisture spatial interpolation, this field of environmental research has significantly matured over the past decades. Despite these considerable developments, point ground soil moisture measurements only provide very limited information both on small- (a few m²) and large-scale (hectares or square kms) soil moisture conditions, especially on terrain of high relief, or uneven vegetation cover.

Besides developing adaptation techniques to global climate changes and altered ecosystem services (Palomo et al. 2017) point measurements and interpolated soil moisture data can be used for many practical applications (Bojovic et al. 2017). Among various uses, some of the most important include (a) agricultural water and irrigation management (b) weather forecasting (Klug – Oana 2015) (c) prediction on fog formation by integrating regional-scale soil moisture into numerical weather models, (d) water balance calculations and estimation of water and solute fluxes and storage in the vadose and root zones, (e) drought forecasting, (f) runoff estimation for flood forecasting, (g) rehabilitation and afforestation projects.

Although remotely sensed data offer unparalleled advantages compared to point ground measurement, it may pose scientific challenges in terms of coarse space and time resolution and shallow penetration depth. Similarly, remotely sensed and ground-measured soil moisture data should be used in a combined manner in order to minimize ambiguity and improve accuracy related to soil moisture measurements.

The findings of our research can be utilized at plot, and small watershed and floodplain scale, in water balance studies. However, since the model presented is still in its initial state and has been developed on soils of silty and clayey-loam texture, calibration and validation runs are needed to test model applicability for other soil physical soil types.

Soil moisture interpolation accuracy depends on site properties and is also influenced by topography, soil and vegetation type as well as the selected interpolation method. Here, in the current study, we selected the ordinary kriging function for interpolation, whereas in the future we plan to test the model with other interpolation methods suggested in multiple former studies (e.g. Zhang et al. 2016) and the one that proves to be the best fit for our validation data. Our results may be inspiring in terms of understanding water dynamics of soils with complex structure. Also, many soil parameters need to be considered in the model, therefore future development is indispensable. Such parameter addition should include organic matter content, and applicability for sandy soils should also be considered in the future. In the current paper, we described homogeneous flow; whereas, in field cases preferential flow may also contribute to subsurface moisture conditions and solute pulses during individual rainstorms as indicated by former studies (e.g. Hendrickx – Flury 2001; Mullane et al. 2015).

Acknowledgement

The authors are grateful to Zoltán Tóth, the director of the ELCOM Kft. for the financial support, Gyula Berki for providing the plot for the current studies and János Kovács for completing the particle size analyses and Gábor Takács and Dávid Ágotha for technical support. The present scientific contribution is dedicated to the 650th anniversary of the foundation of the University of Pécs, Hungary.

5. References

- Anderson, M.G. – Kneale, P.E. (1980): Topography and hillslope soil water relationships in a catchment of low relief. *Journal of Hydrology*. 47 (1-2): 115-128.
- Bárdossy, A. – Lehmann, W. (1998): Spatial distribution of soil moisture in a small catchment. Part 1: geostatistical analysis. *Journal of Hydrology*. 206 (1): 1-15.
- Bojovic, D. – Giupponi, C. – Klug, H. – Morper-Busch, L. – Cojocar, G. – Schörghofer, R. (2017): An online platform supporting the analysis of water adaptation measures in the Alps. *Journal of Environmental Planning and Management*. Published online: 1-16.
- Brocca, L. – Melone, F. – Moramarco, T. – Morbidelli, R. (2009): Antecedent wetness conditions based on ERS scatterometer data. *Journal of Hydrology* 364 (1-2): 73-87.
- Buzás I. (1993): Talaj- és agrokémiai vizsgálati módszertan I. INDA 4231 Kiadó. Budapest (in Hungarian) p. 357.
- Cosh M.H. – Jackson T.J. – Bindlish R. – Pruegger J.H. (2004): Watershed scale temporal and spatial stability of soil moisture and its role in validating satellite estimates. *Remote Sensing of Environment*. 92: 427-435.
- Flint, A.L. – Flint, L.E. (2002): Particle density. In: Dane, J.H. –Topp, G.C. (Eds.)(2002): *Methods of Soil Analysis*. Part 4: Physical Methods. SSSA Book Series No. 5. SSSA. Madison. WI. 229–240.
- Fu B. – Wang J. – Chen L. – Qiu Y. (2003): The effects of landuse on soil moisture variation in the Danangou catchment of the Loess Plateau, China. *Catena*. 54 (1-2): 197-213.
- Gravalos, I. – Moshou, D. – Loutridis, S. – Gialamas, Th. – Kateris, D. – Bompolas, E. – Tsiropoulos, Z. – Xyradakis, P. – Fountas, S. (2013): 2D and 3D soil moisture imaging using a sensor-based platform moving inside a subsurface network pipes. *Journal of Hydrology*. 499: 146-153.
- Heathman, G.C. – Cosh, M.H. – Merwade, V. – Han, E. (2012): Multi-scale temporal stability analysis of surface and subsurface within the Upper Cedar Creek Watershed, Indiana. *Catena*. 95: 91-103.
- Hegedüs, P. – Czigány S. – Pirkhoffer, E. – L. Balatonyi, L. – R. Hickey (2015): Analysis of spatial variability of near-surface soil moisture to increase rainfall-runoff modelling accuracy in SW Hungary. *Open Geosciences* 7(1): 126–139.
- Hendrickx, J.M.H. – M. Flury. (2001): Uniform and preferential flow mechanisms in the vadose zone. In: National Academy Council (2013): *Conceptual models of flow and transport in the fractured vadose zone*. National Academy Press. Washington DC. 149-187.
- Honar, M. R. – Shamsnia S. A. – Gholami A. (2011): Evaluation of water flow and infiltration using HYDRUS model in sprinkler irrigation system. In (2011): 2nd International Conference on Environmental Engineering and Applications. IACSIT Press. Singapore. 17: 276-281.
- Jia, Y.-H. – Shao, M.-A. – Jia, X.-X. (2013): Spatial pattern of soil moisture and its temporal stability within profiles on a loessial slope in northwestern China. *Journal of Hydrology*. 495: 150-161.
- Klug, H. – Oana, L. (2015): A multipurpose weather forecast model for the Mondsee Catchment. *Journal for Applied Geoinformatics*. 1: 602-611.
- Lacava T. – Brocca L. – Calice G. – Melone F., Moramarco T. – Pergola N. – Tramutoil V. (2010): Soil moisture variations monitoring by AMSU-based soil wetness indices: a long-term inter-comparison with ground measurements. *Remote Sensing of Environment*. 114 (10): 2317-2325.
- Loew, A. – Schlenz, F. (2011): A dynamic approach for evaluating coarse-scale satellite soil moisture products. *Hydrology and Earth System Sciences*. 15 (1): 75-90.
- Mualem, Y. 1976. A new model for predicting the hydraulic conductivity of unsaturated porous media. *Water Resources Research*. 12:513-522.
- Mohanty, B.P. – Skaggs, T.H. (2001): Spatio-temporal evolution and time-stable characteristics of soil moisture within remote sensing footprints with varying soil, slope, and vegetation. *Advances in Water Resources*. 24 (9): 1051-1067.
- Makó, A. – Tóth, B. – Hernádi, H. – Farkas, Cs. – Marth, P. (2010): Introduction of the Hungarian Detailed Soil Hydrophysical Database (MARTHA) and its use to test external pedotransfer functions. *Agrokémia és Talajtan*. 59 (1): 29-38.

- Mullane, J.M. – M. Flury – H. Iqbal – P.M. Freeze – C. Hinman – C.G. Cogger – Z. Shi. (2015): Intermittent rainstorms cause pulses of nitrogen, phosphorus and copper in leachate from compost in bioretention systems. *Science of Total Environment*. 537:294-303.
- Novák T. (2005): Afforestations in the Hungarian puszta area: their role in the landscape structure, and influence on the landscape elements. In: *Landscape change, Papers of ECLAS International Conference on Landscape Planning*, Ankara, Turkey. 230-240.
- Novák T. J. – Incze, J. – Rózsa, P. (2013): Quantifying anthropogeomorphological transformation by using the concept of 'hemeromorphy' - a case study from Hungary, the Tokaj Big Hill. In: Novotny, J. – Lehotsky, M. – Raczkowska, Z. – Machova, Z. (Eds.)(2013):*Book of Abstract. Carpatho-Balkan-Dinaric Conference on Geomorphology*, Stara Lesna 2013.06.24-28. *Geomorphologia Slovaca et Bohemica*, Association of Slovak Geomorphologists on the SAS, Czech Association of Geomorphologists, Institute of Geography - Slovak Academy of Sciences. Bratislava. 59.
- Or, D. – Wraith J.M. (2000): Soil water content and water potential relationships. In: Sumner, M.E. (Ed.): *Handbook of Soil Science*. CRC Press, Boca Raton. 1-28.
- Paul, W – Speckmann, H (2004): Radar sensors: emerging technologies for precision farming - Part 1: Basic concepts and soil moisture measurements. *Landbauforschung Volkenrode*. 54 (2): 73-86.
- Penna, D., – Borga, M. – Norbiato, D. – Dalla Fontana, G. (2009): Hillslope scale soil moisture variability in a steep alpine terrain. *Journal of Hydrology*. 364 (3-4): 311-327.
- Perry, M.A. – Niemann, J.D. (2008): Generation of soil moisture patterns at the catchment scale by EOF interpolation. *Hydrology and Earth System Sciences*. 4 (5): 2837-2874.
- Palomo, I. – Bagstad, K.J. – Nedkov, S. – Klug, H. – Adamescu, M. – Cazacu, C. (2017): Tools for mapping ecosystem services. In: Burkhard, B. – Maes, J. (Eds.) (2011): *Mapping Ecosystem Services*. Pensoft Publishers Ltd. Sofia. 52-56.
- Venkatesh, B. – Lakshman, N. – Puranara, B. K. – Reddy, V. B. (2011): Analysis of observed soil moisture patterns under different land covers in Western Ghats, India. *Journal of Hydrology*. 397 (3-4): 281-294.
- Wang, L. – Qu, J. J.(2009): Satellite remote sensing applications for surface soil moisture monitoring: a review. *Frontiers of Earth Science in China*. 3 (2): 237-247.
- Yao, X. – Fu, B. – Lü, Y. – Sun, F. – Wang, S. – Liu, M. (2013): Comparison of Four Spatial Interpolation Methods for Estimating Soil Moisture in a Complex Terrain Catchment. *PLoS ONE*. 8 (1): e54660.
- Zhou, I. – Chen, N. – Chen, Z. (2016): ROSCC: An Efficient Remote Sensing Observation-Sharing Method Based on Cloud Computing for Soil Moisture Mapping in Precision Agriculture. *IEEE Journal of Selected Topics in Applied Earth Observations and Remote Sensing*. 9 (12): 5588-5598.
- Zhu, Q. – Lin, H. (2011): Influences of soil, terrain, and crop growth on soil moisture variation from transect to farm scales. *Geoderma*. 163 (1): 45-54.
- Zhang, J. – Li X., – Liu, Q. – Zhao, L. – Dou, B. (2016): An Extended Kriging method to interpolate soil moisture data measured by wireless sensor network. *Hydrology and Earth System Sciences*.